Journal of Medicinal Chemistry

Article

pubs.acs.org/jmc

Newly Synthesized Curcumin Derivatives: Crosstalk between Chemico-physical Properties and Biological Activity

Erika Ferrari,[†] Francesca Pignedoli,[†] Carol Imbriano,[‡] Gaetano Marverti,[§] Valentina Basile,[‡] Ettore Venturi,[†] and Monica Saladini*[,†]

[†]Department of Chemistry, University of Modena and Reggio Emilia, Via Campi 183, 41125 Modena, Italy

[‡]Department of Biology, University of Modena and Reggio Emilia, via Campi 213/D, 41125 Modena, Italy

[§]Department of Biomedical Science, University of Modena and Reggio Emilia, Via Campi 287, 41125 Modena, Italy

Supporting Information

ABSTRACT: New curcumin analogues (ester and acid series) were synthesized with the aim to improve the chemical stability in physiological conditions and potential anticancer activity. Cytotoxicity against different tumorigenic cell lines (human ovarian carcinoma cells −2008, A2780, C13*, and A2780/CP, and human colon carcinoma cells HCT116 and LoVo) was tested to evaluate cellular specificity and activity. Physico-chemical properties such as acidity, lipophilicity, kinetic stability, and free radical scavenging activity were investigated to shed light on the structure−activity relationship and provide new attractive candidates for drug development. Most of ester derivatives show IC_{50} values lower than curcumin and exhibit selectivity against colon carcinoma cells. Especially they are extremely active after 24 h exposure showing enhanced inhibitory effect on cell viability. The best performances of ester curcuminoids could be ascribed to their high lipophilicity that favors a greater and faster cellular uptake overcoming their apparently higher instability in physiological condition.

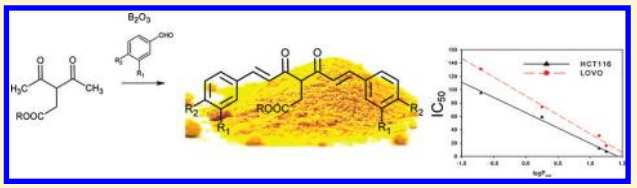

1. INTRODUCTION

Medicinal plants have been an excellent source of pharmaceutical agents for a long time. Curcuminoids are natural yellow pigments and food-coloring agents present in the rhizomes of the Asian tropical plant *Curcuma longa* L., which has been used as a traditional medicinal herb for thousands of years. The dried rhizome of *C. longa* has been widely used as an aromatic stomachic, carminative, anthelmintic, laxative, as well as for liver ailments and as condiment in foods. Curcumin, 1,7-bis(4-hydroxy-3-methoxyphenyl)-1,6-heptadien-3,5-dione, is the primary bioactive compound isolated from this spice.

In the past decade, a large number of reports have been published on the beneficial effects of curcumin, and it has repeatedly been claimed that this natural product is efficient and safe for the prevention and treatment of several diseases including cancer.[1,2]

Curcumin inhibits cell proliferation of a variety of transformed cell types, including T- and B-cell lymphomas, breast, colon, gastric, ovarian, prostate, and oral epithelial carcinoma cells.[3] Moreover, its cytotoxic activity is confined to cancer cells, thus promising low side effects of anticancer drugs based on curcumin structure. Although numerous studies have been performed, the origins of the curcumin anticancer effect have not been elucidated yet. Curcumin acts by a multitude of different mechanisms and targets multiple proteins, both directly and indirectly, including transcription factors (NF-kB, STAT3, Egr-1, AP-1, PPAR-γ, β-catenin), coactivators and corepressors (p300/CBP, HDAC1), and genes regulating apoptosis (p53, Bcl-2, Bcl-xL, Bax).[4]

A robust activity of curcumin was described in colon cancers, showing the safety and tolerability of curcumin in patients with colorectal carcinoma diseases.[5] Curcumin inhibits proteasome activity,[6] exhibits changes in cell cycle progression,[7] and induces apoptosis in HCT116 cells, a human colon carcinoma cell line.[8] Cells growth inhibition, cell cycle arrest in G2/M phase, and apoptotic cell death were also observed in other human colon cancer cells, LoVo, SW480, and HCT15.[9]

In addition, it has been shown that curcumin induces apoptosis in ovarian carcinoma OVCA429 and SKOV3 cells[10] and that it is also able to increase sensitivity of both wild type and cisplatin (cDDP) resistant ovarian cancer cells.[11] We have previously reported that the cDDP-resistant human ovarian carcinoma cell line, C13*, was also cross-resistant to curcumin in comparison with the parental-sensitive cell line, 2008.[12] In fact, the observed resistant factor (RF = IC_{50} resistant/IC_{50} parent line)[13] was 3.4 toward curcumin.

Unlike most chemotherapeutic agents, curcumin shows little to no toxicity (no dose-limiting toxicity at doses up to 10 g/day in humans),[14] but no human studies were conducted to test the dose levels which cause long-term toxicity so far.

However, clinical use of curcumin is severely limited by its extremely low bioavailability, which is a consequence of poor

Received: July 4, 2011
Published: October 27, 2011

solubility and instability in aqueous solution, in particular at alkaline pH.[15,16]

As far as cancer is concerned, in vitro studies have demonstrated that cancer cells do not die unless they are exposed to curcumin concentrations of 5−50 μM for several hours.[17,18] Because of its poor bioavailability, these concentrations are not achieved outside the gastrointestinal tract when curcumin is taken orally. Several reports have shown that the concentrations of curcumin in plasma of people taking relatively high oral doses are very low, typically in the nanomolar range,[17] hence its anticancer activity may be limited to gastrointestinal tract.[19] In addition, its limited bioavailability and extensive metabolism suggest a possible disagreement between anticancer effects observed in vitro and its in vivo activity.[17]

To overcome the low oral bioavailability of curcumin, several strategies have been proposed[20] such as complexation with cyclodextrin,[16] conjugation with nucleosides,[21] biopolymers,[22] and composite nanoparticles.[23] One of these strategies has entered clinical trials and consists of using the black pepper alkaloid piperine (bioperine) to increase the bioavailability of curcumin.[24] Besides, numerous analogues of curcumin have been synthesized and tested to investigate their activity against known biological targets to improve the pharmacological profile of the natural product (i.e., improve their selectivity, bioavailability, and stability).[25,26] Recently, the introduction of glycoside moiety at the phenyl ring of curcumin was found to enhance its water solubility and chemical stability.[12] In this case, the substitution of the mobile phenolic hydrogens gave compounds with no gain in antiproliferative activity with respect to curcumin.

In this scenario, we have here designed and synthesized new curcumin analogues (Figure 1) in which we have modified the

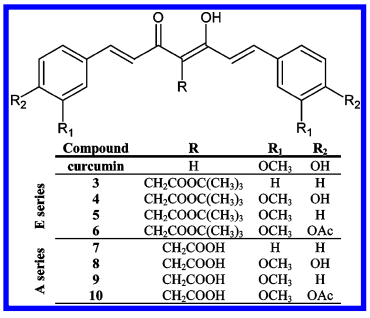

	Compound	R	R_1	R_2
	curcumin	H	OCH_3	OH
E series	3	$CH_2COOC(CH_3)_3$	H	H
	4	$CH_2COOC(CH_3)_3$	OCH_3	OH
	5	$CH_2COOC(CH_3)_3$	OCH_3	H
	6	$CH_2COOC(CH_3)_3$	OCH_3	OAc
A series	7	CH_2COOH	H	H
	8	CH_2COOH	OCH_3	OH
	9	CH_2COOH	OCH_3	H
	10	CH_2COOH	OCH_3	OAc

Figure 1. Structures of curcumin and newly synthesized curcuminoids.

β-keto-enolic moiety, inserting an alkylic group with the aim to improve the chemical stability in physiological conditions and the potential anticancer activity with respect to the parent compound. Cytotoxicity against different tumorigenic cell lines (cisplatin-sensitive human ovarian carcinoma cell lines 2008 and A2780, compared with their respective -resistant counterparts, C13* and A2780/CP cells, and human colon carcinoma cell lines, HCT116 and LoVo) is tested with the purpose of evaluating possible specificity and selectivity of the new compounds. Furthermore, results from in vitro biological assays are here related to chemico-physical properties such as acidity, lipophylicity, kinetic stability, and free radical scavenging activity in order to shed light on structure−activity relationship and supply new attractive candidates for drug development.

2. RESULTS AND DISCUSSION

2.1. Synthesis of Curcuminoids. In the present study, we have synthesized new curcumin derivatives (Figure 1) in order to investigate the effect of the insertion of an alkylic chain on the β-keto-enolic moiety (C3 substitution) both on physico-chemical properties and biological activity. We decided to add a short chain to keep low the molecular weight. To understand the role of polarity and acidity in relation to biological activity, we investigated both ester and acid derivatives, here named **E** and **A** series, respectively. We tested different ester protecting groups (data not shown), but in many cases deprotection conditions led to the breakage of curcumin backbone, and for this reason we chose to protect the carboxyl with Boc function which could be removed with no degradation of curcumin structure.

Four differently substituted benzaldehydes were chosen to investigate the role of electronic effects and intramolecular hydrogen bond on chemical and biological properties.

E and **A** series, except of compound **8**, were synthesized from **1** (route ***a***, Scheme 1) employing the renowned Pabon reaction[27] under modified conditions as previously reported by the authors for curcumin.[7] Acetylacetonate−boron complex is formed with the aim of activating the methyl positions of 2,4-pentanedione for aldol condensation and preventing Knoevenagel condensation the on methylene group. The required condensation product is set free from boron by addition of an acid aqueous solution. We have optimized the reaction conditions of route ***a*** with respect to the previously investigated substituted curcuminoids.[26,28,29]

In route ***a***, compounds **3**−**6** were obtained using DMF instead of EtOAc, the commonly used solvent for Pabon reaction, in view of its ability to provide: (i) high solubility of reactants and intermediates, (ii) suitable polarity for the process, and (iii) easy reaction workup, particularly the isolation and separation of curcuminoids from byproduct. To maintain satisfactory reaction yields, the aldol condensation reaction is carried out under anhydrous conditions, and tributylborate (n-BuO)$_3$B is added as drying agent. On the whole, this one-pot reaction is characterized by quite good yields (~65%), short time (6 h), and small volumes of solvents (1 mL DMF/0.5 mmol product). The following deprotection of Boc group affords the acid derivatives **7**, **9**, and **10**. Compound **8** is unstable under the reaction conditions employed for Boc deprotection (50% TFA in CH_2Cl_2 at 0 °C); for this reason a new strategic synthetic pathway (route ***b***, Scheme 1) was used. Defferently from route ***a***, Boc group deprotection was performed before aldol condensation.

According to route ***b***, curcumin derivative **8** was prepared directly from **2** in reaction condition similar to those reported by Babu.[30]

The choice of Boc deprotection as the first step in route ***b*** allows obtaining compound **8** in milder acidic conditions, overcoming its instability. The synthetic pathway ***b*** was also tested to synthesize compound **7**, **9**, and **10** but reaction yields were significantly lower than those achieved by route ***a***.

2.2. X-ray Crystallography. ORTEP[31] view of **5** structure is reported in Figure 2, geometric parameters are reported in Table 1. The compound is in the keto-enolic form with a strong intramolecular hydrogen bond [O1−H1 1.05(6) Å, O1···O2 2.428(5) Å, H1···O2 1.4386) Å, O1−H1···O2 158(4)°].

Although the presence of a bulky electron-withdrawing group on the central carbon in β-diketones was found stabilizing the

dx.doi.org/10.1021/jm200872q | J. Med. Chem. 2011, 54, 8066−8077

Scheme 1. General Synthetic Strategies for Symmetric Curcumin Analogues[a]

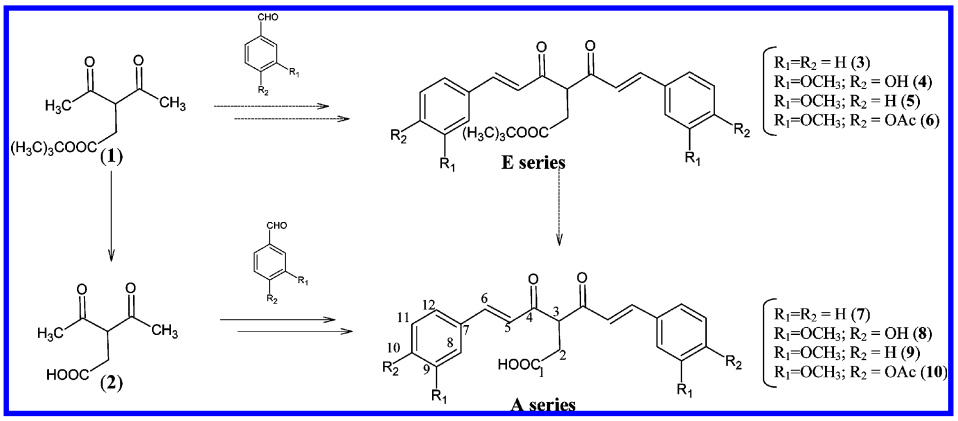

[a]The two different investigated routes, ***a*** and ***b***, are represented with dotted and solid arrows respectively.

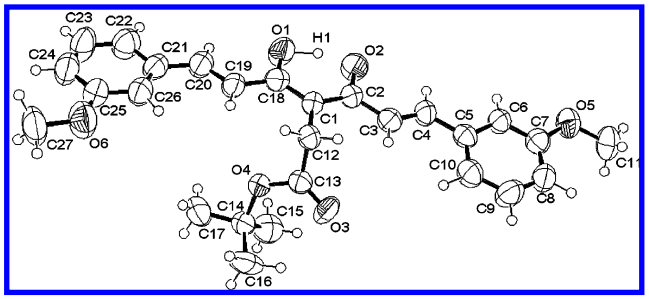

Figure 2. ORTEP view of compound **5**.

diketo form,[32] the considerable charge delocalization over the whole framework contribute to stabilize the keto-enolic tautomer. This behavior was previously found for curcumin in the solid state[33] and for its derivatives.[34] The geometry around C1 indicates an sp^2 coordination, as expected for the keto-enol tautomer.

2.3. Acidity. pH-Metric titrations were performed by means of UV−vis spectroscopy on **A** compounds in order to assess their acidity and predict the most abundant species in physiological pH range. All the compounds undergo a tautomeric equilibrium (Scheme 2) which is highly solvent dependent. Anyway, the prevailing tautomer for both **E** and **A** families in physiological condition is the diketo form, as suggested by the value of λ_{max} around 320 nm in UV−vis spectra;[35] the opposite takes place in aprotic/apolar solvents, in which the keto-enolic tautomer is the most abundant, as shown by NMR data (Experimental Section).

Increasing pH, simultaneous equilibria, involving keto-enolic tautomerism and acid dissociations, take place, giving rise to a intricate titolative spectral pattern (Figure 3). Despite this apparent complex behavior, for all **A** molecules, the plot of absorbance at λ_{max} vs pH shows titolative trend characterized by two equivalent points: the first (pH ∼ 4.5) corresponds to the dissociation of carboxyl group and the second one (pH ∼ 9) is due to the keto-enol deprotonation. Overall protonation constants were calculated from spectrophotometric data and optimized by means of pHab software,[36] and log β and pK_a values are summarized in Table 2. The carboxylic pK_a value is similar for all the compounds, while the enolic dissociation is strongly influenced by the electron withdrawing effect of the aromatic substituents, in the order of increasing acidity **7** < **9** < **10** < **8**, a similar behavior was previously observed for other curcuminoids substituted on the aromatic ring as reported by Caselli et al.,[35] Ferrari et al.,[12] and references cited therein. As shown by the species distribution curves (Figure 4), the prevailing species at physiological pH (7.4) is the monodissociated

Table 1. Bond Lengths [Å] and Angles [deg] for Compound 5

O(1)−C(18)	1.293(4)	C(6)−C(7)	1.377(6)
O(2)−C(2)	1.299(4)	C(7)−C(8)	1.369(6)
O(3)−C(13)	1.194(4)	C(8)−C(9)	1.378(6)
O(4)−C(13)	1.335(5)	C(9)−C(10)	1.375(6)
O(4)−C(14)	1.478(5)	C(12)−C(13)	1.506(6)
O(5)−C(7)	1.371(5)	C(14)−C(15)	1.500(7)
O(5)−C(11)	1.424(6)	C(14)−C(17)	1.503(6)
O(6)−C(25)	1.368(5)	C(14)−C(16)	1.514(6)
O(6)−C(27)	1.430(6)	C(18)−C(19)	1.464(6)
C(1)−C(2)	1.398(5)	C(19)−C(20)	1.311(5)
C(1)−C(18)	1.403(5)	C(20)−C(21)	1.464(6)
C(1)−C(12)	1.525(5)	C(21)−C(26)	1.381(6)
C(2)−C(3)	1.452(6)	C(21)−C(22)	1.386(6)
C(3)−C(4)	1.318(5)	C(22)−C(23)	1.379(7)
C(4)−C(5)	1.468(6)	C(23)−C(24)	1.361(7)
C(5)−C(6)	1.381(5)	C(24)−C(25)	1.366(6)
C(5)−C(10)	1.385(6)	C(25)−C(26)	1.376(6)
C(13)−O(4)−C(14)	121.9(3)	O(3)−C(13)−C(12)	124.0(4)
C(7)−O(5)−C(11)	118.0(4)	O(4)−C(13)−C(12)	110.9(4)
C(25)−O(6)−C(27)	118.5(5)	O(4)−C(14)−C(15)	109.9(3)
C(2)−C(1)−C(18)	119.2(4)	O(4)−C(14)−C(17)	101.9(4)
C(2)−C(1)−C(12)	120.0(4)	C(15)−C(14)−C(17)	110.7(5)
C(18)−C(1)−C(12)	120.8(4)	O(4)−C(14)−C(16)	109.5(4)
O(2)−C(2)−C(1)	120.8(4)	C(15)−C(14)−C(16)	112.5(4)
O(2)−C(2)−C(3)	115.4(4)	C(17)−C(14)−C(16)	111.8(4)
C(1)−C(2)−C(3)	123.8(4)	O(1)−C(18)−C(1)	120.5(4)
C(4)−C(3)−C(2)	123.8(4)	O(1)−C(18)−C(19)	114.8(5)
C(3)−C(4)−C(5)	127.5(4)	C(1)−C(18)−C(19)	124.7(5)
C(6)−C(5)−C(10)	118.1(4)	C(20)−C(19)−C(18)	123.3(5)
C(6)−C(5)−C(4)	119.4(4)	C(19)−C(20)−C(21)	127.8(5)
C(10)−C(5)−C(4)	122.5(4)	C(26)−C(21)−C(22)	117.9(5)
C (7)-C(6)−C(5)	121.8(4)	C(26)−C(21)−C(20)	122.5(5)
C(8)−C(7)−O(5)	123.9(5)	C(22)−C(21)−C(20)	119.6(5)
C(8)−C(7)−C(6)	120.1(4)	C(23)−C(22)−C(21)	120.2(5)
O(5)−C(7)−C(6)	116.0(5)	C(24)−C(23)−C(22)	121.1(5)
C(7)−C(8)−C(9)	118.3(5)	C(23)−C(24)−C(25)	119.3(5)
C(10)−C(9)−C(8)	122.2(5)	C(24)−C(25)−O(6)	123.8(6)
C(9)−C(10)−C(5)	119.5(4)	C(24)−C(25)−C(26)	120.3(5)
C(13)−C(12)−C(1)	113.8(4)	O(6)−C(25)−C(26)	115.9(5)
O(3)−C(13)−O(4)	125.1(4)	C(21)−C(26)−C(25)	121.2(5)

dx.doi.org/10.1021/jm200872q|J. Med. Chem. 2011, 54, 8066−8077

Scheme 2. General Scheme of Tautomeric Equilibrium between Keto-enolic (KE) and Di-ketonic (DK) Forms of New Curcumin Analogues E and A

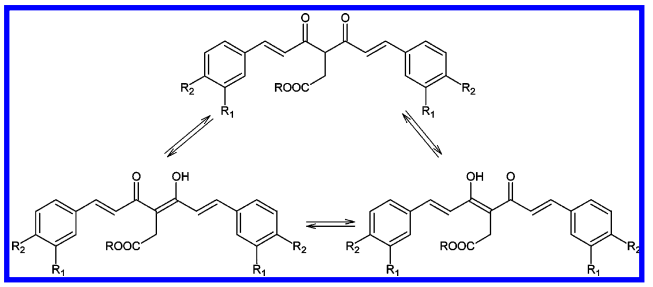

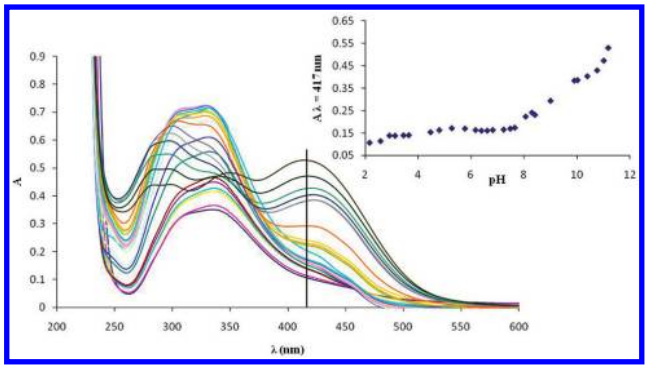

Figure 3. pH-Metric spectrophotometric titration of **10**; the insert shows the plot of absorbance (A) vs pH at λ_{max} = 417 nm.

Table 2. Logarithm of Protonation Constants ($\log\beta_{LH}$) and pK_a Values Calculated with pHab[36] from Spectrophotometric Titrations Performed at 25 °C, I = 0.1 M ($NaNO_3$)

	7	8	9	10
$\log\beta_{11}$	10.46(1)	13.35(1)	9.44 (4)	9.04(1)
$\log\beta_{12}$	15.10(4)	22.98(2)	14.52 (2)	13.47(1)
$\log\beta_{13}$		31.40(1)		
$\log\beta_{14}$		35.84(1)		
pK_{a1}	4.54(5)	4.44(5)	5.08(6)	4.43(2)
pK_{a2}	10.46(1)	8.42(4)	9.44(4)	9.04(1)
pK_{a3}		9.63(3)		
pK_{a4}		13.35(1)		

one for all **A** compounds. Anyway for **8** about 15% of the dianionic species is present as well.

The investigation on the acidity of **E** compounds was precluded by the low stability in basic condition of Boc group, therefore it is not possible to determine enolic pK_a, which is the only acid moiety. Assuming that this value is ∼9, as found in **A** compounds, it is reasonable to assess that the most abundant species is the neutrally charged one in physiological condition.

2.4. Kinetic Stability. In the present investigation, we want to test if the introduction of an alkylic chain on C-3 position of curcumin backbone can improve stability in physiological conditions. In fact, several pharmacokinetics studies on curcumin showed that its main drawbacks are the extremely fast degradation and its extensive metabolism that both induce particularly low plasma concentration, typically in the nanomolar range.[19] Figure 5 reports the decomposition kinetics profiles of **A** and **E** compounds in simulated physiological conditions (parts A and B) and their linear fittings[37] (parts C and D). Table 3 summarizes hyperbolic function parameters ($\boldsymbol{a}$ and $\boldsymbol{b}$) together with their reciprocal values and statistical parameter R^2. The reciprocal of $\boldsymbol{a}$ ($\mathbf{1}/\boldsymbol{a}$) corresponds to the minimum percentage of residual compound achieved in physiological condition. The value ($-\mathbf{1}/\boldsymbol{b}$) is related to the degradation rate: the higher the value the faster the degradation process. Compounds **7** and **9** show the highest values for $\mathbf{1}/\boldsymbol{a}$ corresponding to the more stable compounds. **10** is characterized by the lowest values of $\mathbf{1}/\boldsymbol{a}$ and $-\mathbf{1}/\boldsymbol{b}$ in fact decomposes up to ∼25% in 8 h, while **8** decomposes quite rapidly up to ∼20% during the first 2 h, showing the highest value of kinetic rate ($-\mathbf{1}/\boldsymbol{b}$). These data point out a strong relationship between the aromatic substituents and kinetics profiles, in particular, the absence of *para* substitution seems to be fundamental in order to achieve stability, while the *meta* group looks like of minor importance. Moreover, the possibility to form an intramolecular hydrogen bond, such as for **8**, appears the driving force in the decomposition process, as observed for curcumin in comparison with derivatives substituted on the aromatic ring.[7] Anyway, compound **8** is more stable than curcumin, as after 2 h it is only 20% degraded vs 40% of curcumin,[12] therefore C-3 substitution on keto-enolic moiety seems to be a key factor in slowing the degradation process of curcuminoids.

E compounds decompose more than their analogues **A**, reaching a residual percentage beneath 50% even though with slower rates as shown by $-\mathbf{1}/\boldsymbol{b}$ values, which are on average minor than their carboxylic counterparts.

This apparent instability of **E** series may be due to the presence of Boc group, which can hydrolyze in slightly basic

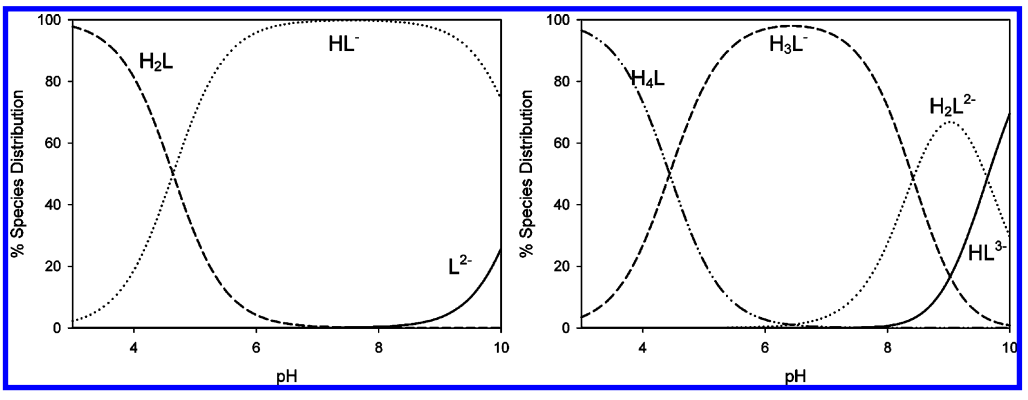

Figure 4. Species distribution curves for **7** (left) and **8** (right), $[L]_{total} = 5 \times 10^{-3}$ M.

dx.doi.org/10.1021/jm200872q | J. Med. Chem. 2011, 54, 8066–8077

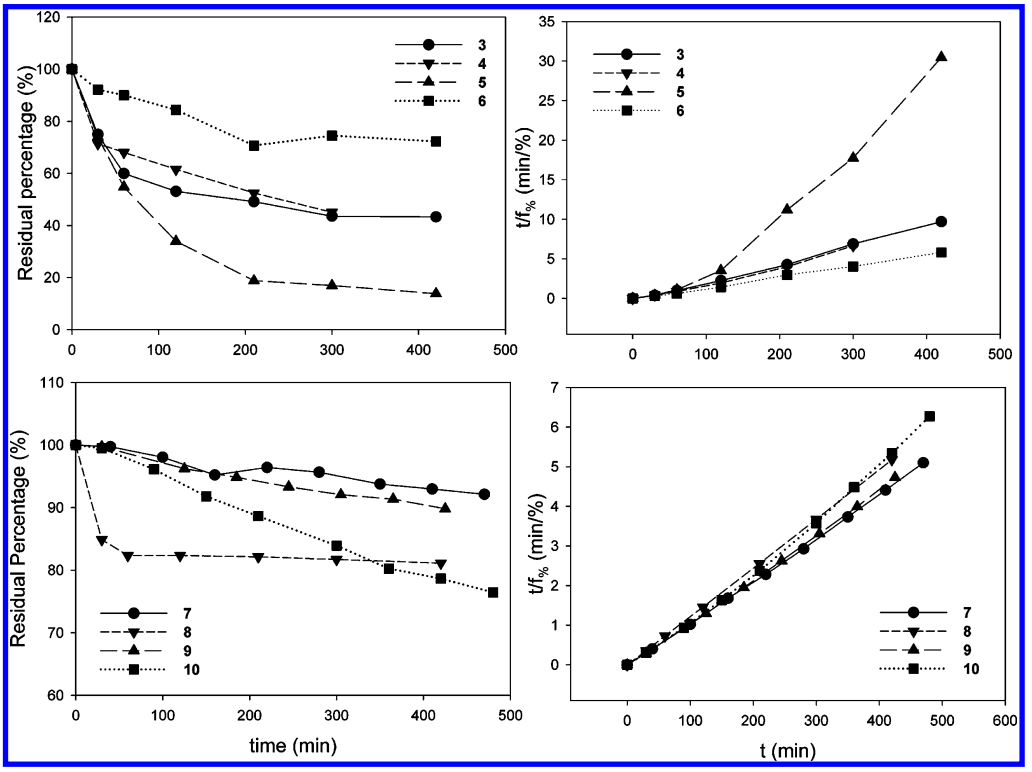

Figure 5. (A,B) Decomposition kinetics profiles of **E** and **A** compounds in buffered aqueous solution (TRIS-HCl pH = 7.4) at 37 °C in darkness over a period of 8 h. Residual concentration is expressed as percentage with respect to concentration at *time zero*. Concentrations were determined by reading absorbance at 300 nm. (C,D) Linearization of kinetics profiles of **A** and **E** compounds by the hyperbolic function $t/f_{\%} = at + b$, where t is time (min) and $f_{\%}$ represents concentration as residual percentage.

Table 3. Linear Fittings for Kinetics Profiles Obtained Using the Function: $t/f_{\%} = at + b$[a]

compd	a	$(1/a)$	b	$(-1/b)$	R^2
3	0.0236	42.37	−0.3353	2.98	0.9958
4	0.022	45.45	−0.3257	3.07	0.9851
5	0.0729	13.72	−2.6655	0.38	0.9679
6	0.0141	70.92	−0.1195	8.37	0.9975
7	0.0108	92.59	−0.0501	19.96	0.9995
8	0.0123	81.30	−0.0143	69.93	0.9999
9	0.0111	90.09	−0.0562	17.79	0.9993
10	0.0131	76.34	−0.1934	5,17	0.9959

[a]Equation parameters (**a** and **b**) and statistical parameter R^2 were extracted by a least-squares fitting on the experimental UV-Vis results.

condition. Anyway, at physiological pH, they have a kinetic stability comparable with curcumin.[12]

2.5. Lipophilicity. The primary property for orally active drugs is the ability to be efficiently absorbed from the gastrointestinal tract (GIT) and to cross biological membranes. The molecular size is a critical factor which influences the rate of drug absorption. The "cutoff" molecular weight for the paracellular route in the human small intestine is 500 Da,[38] and A and E molecules are talented with this prerequisite. In addition, lipophilicity, which is usually quantified by the logarithm of the 1-octanol/water partition coefficient (log P_{oct}), is a fundamental chemico-physical factor, because it is correlated to permeability and drug penetration into cells and into the central nervous system.[39] To achieve efficient oral absorption, log P_{oct} should be greater than −0.7[40] and lower than 5.[38] For all the synthesized curcuminods we can potentially predict good absorption and permeation because they satisfy the Lipinski's "rule of 5": there are less than 5 H-bond donors, MW is lower than 500 Da, log P is <5, and there are less than 10 H-bond acceptors.[38]

Table 4 reports log P_{oct} and water-solubility values, which show inverse proportionality. **8** and **10** exhibit the lower log P_{oct}; this seems to be related to their higher acidity with respect to **9** and **7**. In particular, **8**, in which the enolic function is partially dissociated at physiological condition, displays an extremely high water solubility and the lowest log P_{oct}. As a consequence, with the exception of **8**, we can expect effective penetration of the drug into cells for all **A** derivatives. **E** compounds demonstrated a great lipophilicity, which prevented log P_{oct} measurement; therefore also for these molecules we can suggest a good cell permeability.

Table 4. Summary of Experimental Physico-Chemical Properties of New Curcuminoids: log P (Logarithm of Partition Coefficient Defined As the Concentration Ratio of Each Compound in *n*-Octanol and Aqueous Buffer Solution, pH = 7.4 and Solubility (mM)[a]

compd	log P	solubility
7	1.14 ± 0.08	0.92 ± 0.02
8	−0.7 ± 0.1	>100
9	1.25 ± 0.05	0.55 ± 0.02
10	0.25 ± 0.02	1.60 ± 0.01

[a]The mean value of three independent experiments ± SD is reported.

2.6. Free Radical Scavenging Ability. The free radical scavenging ability of synthesized curcuminoids was evaluated by the DPPH radical assay, which is one of the most widely used

dx.doi.org/10.1021/jm200872q | J. Med. Chem. 2011, 54, 8066–8077

method to determine antioxidant activity. Results, summarized in Figure 6, point out that curcuminoids can be divided into two main groups according to their DPPH inhibition, expressed as EC_{50} (the antioxidant concentration necessary to decrease the initial amount of DPPH by 50%). **4** and **8** show EC_{50} values of 16 ± 1 μM and 11 ± 1 μM, respectively, which are close to that of curcumin (13 ± 1 μM). For all the other compounds, EC_{50} is not reached within 1/1 molar ratio.

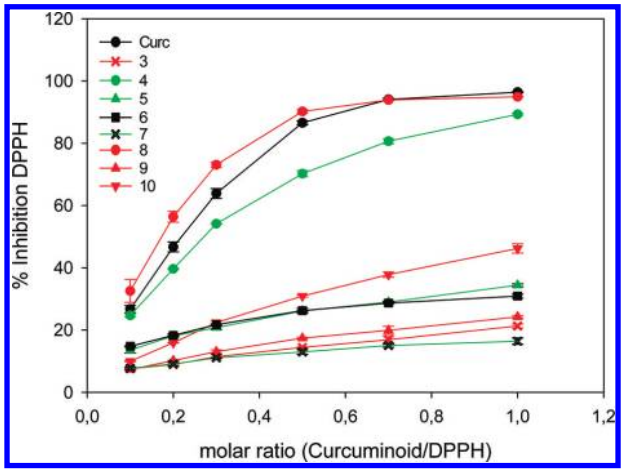

Figure 6. The percentage inhibition of free DPPH radical in presence of different curcuminoids; curcuminoid concentration is expressed as molar ratio (mol of curcuminoid/mol of DPPH).

Some studies on antioxidant properties of curcumin[41] highlighted a mechanism involving H-atom transfer from the keto-enolic moiety, excluding the extraction of phenolic H-atoms due to their participation in intramolecular H-bonds with adjacent methoxyl groups. On this basis, we should predict similar free radical scavenging ability for all our compounds; on the contrary, our findings evidenced a significant inhibition of DPPH only for those compounds characterized by the presence of phenolic groups (**4** and **8**), therefore we suggest that the mechanism of H-transfer originates mainly from phenolic groups rather than from keto-enolic moiety; in this way phenolic OH groups are mainly responsible for antioxidant activity of curcumin confirming the mechanism suggested by Priyadarsini et al.[42]

2.7. Biological Assays. The effectiveness of curcumin and curcuminoids against human ovarian and colon carcinoma cell lines, expressed as IC_{50} values, are reported in Table 5.

With the exception of **8** and **10**, all compounds show IC_{50} values after 72 h treatment equal or lower than curcumin on cDDP-sensitive human ovarian carcinoma cells. As already reported, the cDDP-resistant counterpart C13* is cross-resistant to curcumin.[12] In addition, we display now that this effect occurs in a time-dependent manner because it increases with the exposure time. Our compounds do not show such cross-resistance, giving similar cell growth inhibition in both 2008 and C13*cell lines; in addition they are all more effective even than curcumin. Of note, **9** is the most potent cell growth inhibitor toward this cDDP-sensitive and -resistant cell model after 48 h treatment. Drug accumulation is the result of uptake and efflux from cells, and many resistant cells expel the drug through the multidrug resistance (MDR) pump,[43] and even cDDP-resistant cells exploit it to extrude most of the drugs.[44] The expression of *mdr*-1 is enhanced in a dose-dependent manner as a series of bladder transitional carcinoma cells acquires progressive cDDP-resistance, indicating a possible role of multidrug resistance-associated protein (MRP).[45] Physical characteristics commonly seen in drugs showing MDR[46] may suggest that most of the compounds could become substrates of P170, the product of *mdr*-1 gene, and so be expelled from

Table 5. IC_{50} Values (μM) for Curcumin and Its Eight Derivatives against Two cDDP-Sensitive Human Ovarian Carcinoma Cell Lines (2008, A2780) and Their Resistant Counterparts (C13*, A2780/CP) and Two Human Colon Carcinoma Cell Lines (HCT116, LoVo)[a]

cell line	*t* (h)	CURC	3	4	5	6	7	8	9	10
2008	24	18 ± 1	18 ± 2	55 ± 7	23 ± 4	34 ± 5	32 ± 4	>100	14 ± 1	72 ± 8
	48	7 ± 1	15 ± 4	35 ± 4	6.9 ± 0.3	18 ± 3	17 ± 3	98 ± 9	6.8 ± 0.4	66 ± 8
	72	4.7 ± 0.5	3.1 ± 0.6	9.6 ± 0.2	2.1 ± 0.4	1.1 ± 0.2	2.5 ± 0.3	70 ± 8	2.0 ± 0.4	24 ± 3
C13*	24	26 ± 3	25 ± 4	49 ± 6	16 ± 2	32 ± 4	25 ± 2	95 ± 11	11 ± 1	>100
	48	18 ± 2	17 ± 4	50 ± 6	11 ± 1	16 ± 2	16 ± 3	99 ± 9	8 ± 1	80 ± 11
	72	16 ± 2	2.5 ± 0.4	10 ± 1	2.6 ± 0.3	3.1 ± 0.4	3.5 ± 0.3	100 ± 11	3.5 ± 0.2	60 ± 5
A2780	24	38 ± 5	40 ± 6	9.4 ± 0.4	9 ± 1	76 ± 8	40 ± 3	>100	17 ± 2	>100
	48	12 ± 1	41 ± 2	7 ± 1	5.8 ± 0.4	28 ± 5	36 ± 8	>100	9 ± 1	>100
	72	8 ± 1	9 ± 1	6.4 ± 0.4	8 ± 1	4 ± 1	10 ± 1	54 ± 7	7 ± 1	46 ± 8
A2780/CP	24	28 ± 3	>100	9 ± 1	8 ± 1	>100	>100	>100	21 ± 2	>100
	48	18 ± 2	39 ± 7	6.3 ± 0.5	6 ± 1	35 ± 6	24 ± 6	>100	10 ± 1	>100
	72	11 ± 2	13 ± 1	7 ± 1	5.3 ± 0.1	5 ± 1	9 ± 1	91 ± 3	7 ± 1	47 ± 6
HCT116	24	13 ± 1	5 ± 1	3.6 ± 0.6	3.5 ± 0.4	3 ± 1	17 ± 3	>100	14 ± 1	56 ± 9
	48	4 ± 2	3.6 ± 0.4	2.3 ± 0.6	2.7 ± 0.8	2.7 ± 0.3	13 ± 2	93 ± 17	8 ± 1	60 ± 10
LoVo	24	16 ± 2	8 ± 2	4.1 ± 0.4	4.6 ± 0.4	4.2 ± 0.5	27 ± 6	>100	20 ± 2	>100
	48	10 ± 1	3.9 ± 0.3	7 ± 1	4.0 ± 0.2	3.5 ± 0.3	26 ± 4	>100	17 ± 1	71 ± 17

[a]The IC_{50} is defined as the concentration causing 50% growth inhibition in treated cells when compared to control cells after 24, 48 or 72 h drug exposure. Values are means ± SD of five separate experiments performed in duplicate.

dx.doi.org/10.1021/jm200872q | J. Med. Chem. 2011, 54, 8066–8077

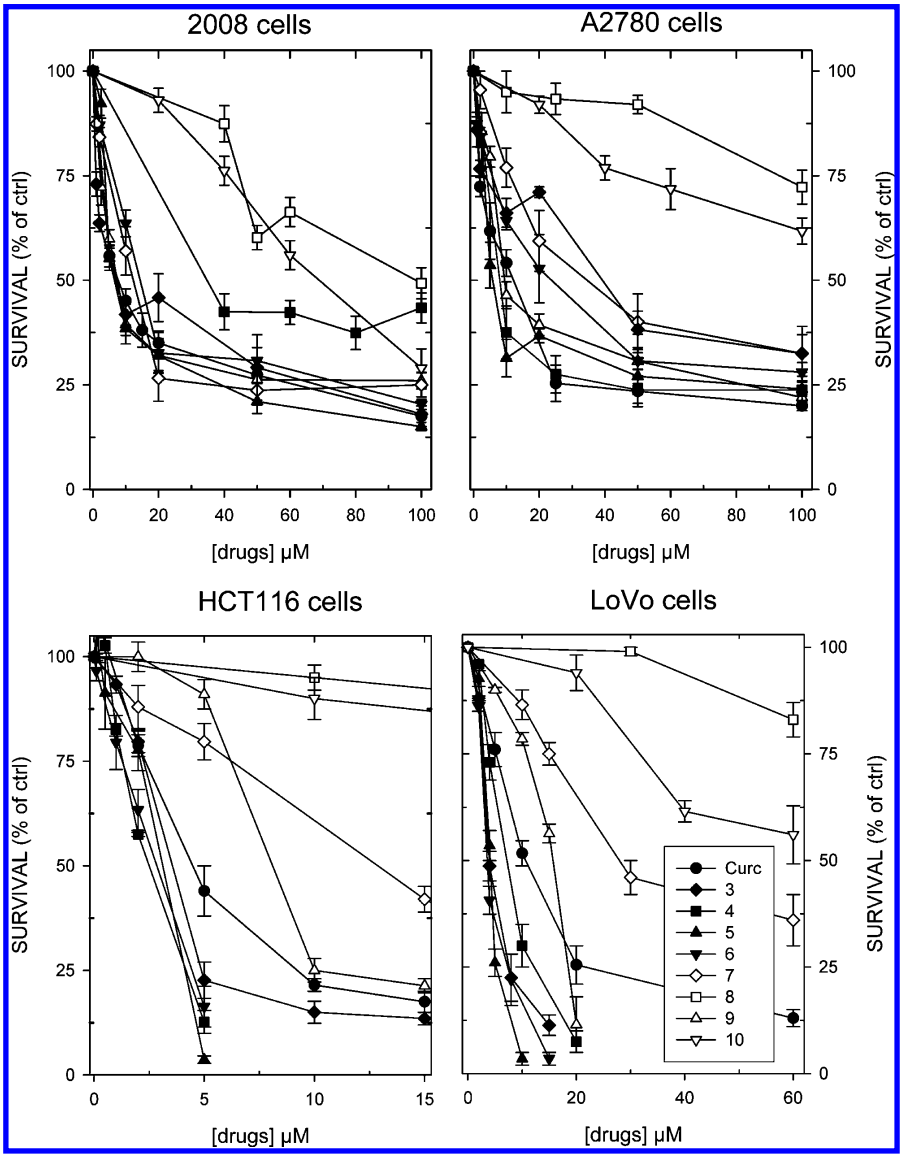

Figure 7. Dose–response curves of curcumin and its eight derivatives against 2008, A2780, HCT116, and LoVo cell lines. Twenty-four h after seeding, ovarian cancer cells (upper panels) and colon cancer cells (lower panels) were exposed to the indicated concentrations of the drugs (open symbols, **A** series; closed symbols, **E** series) for 48 h and then stained with crystal violet solution. Results represent the mean of three separate experiments performed in duplicate. Error bars, SEM.

resistant cells, accounting for the impairment of drug accumulation and cross-resistance.

On the contrary, in the other couple of ovarian cancer cell lines, A2780 and A2780/CP, no cross-resistance was observed toward both curcumin and its derivatives; probably, these cell lines accumulate equal amounts of each compound that could also undergo the same biotransformation. In addition, because cDDP-resistance in C13* cells has been partly related to mitochondria alterations raised during resistance selection,[47] and never reported in A2780/CP cells, it could be suggested that these mitochondrial defects in C13* cells may impair curcumin and its derivatives effects on these organelles.[48]

A time-dependent behavior is observed only for curcumin and the less active compounds on ovarian carcinoma cell lines A2780 and A2780/CP, while the more cytotoxic ones (**4**, **5**, **9**) manifest a cell growth inhibition at 24 h exposure similar or lower than the one obtained with curcumin after 72 h.

In addition, from Table 5, it is also evident that 2008 and C13* cells are more responsive to both curcumin and most of its derivatives with respect to A2780 and A2780/CP. On the contrary, compounds **4** and **5** result more cytotoxic against the latter cells than the former ones.

Curcumin derivatives were also tested on human colon carcinoma cell lines (HCT116 and LoVo) (Table 5), displaying in general lower IC_{50} values than those gained against human ovarian carcinoma cells previously discussed. Differently from curcumin, which showed a time-dependent inhibitory activity on cells doubling, the synthesized derivatives did not lower their IC_{50} values with prolonged exposure, as indicated by the comparison between 24 h and 48 h treatments. This phenomenon could be the consequence of a rapid cellular uptake along with a fast metabolic degradation.

Figure 7 depicts the dose–response curve of curcumin and its eight derivatives, in two cDDP-sensitive human ovarian carcinoma cell lines (parts A and B) and two colon cancer cell lines (parts C and D) after 48 h exposure, corresponding to about two cell cycle span. As it appears, most of the drugs killed more than 70% of 2008 cells within 25 μM, or at

dx.doi.org/10.1021/jm200872q | J. Med. Chem. 2011, 54, 8066–8077

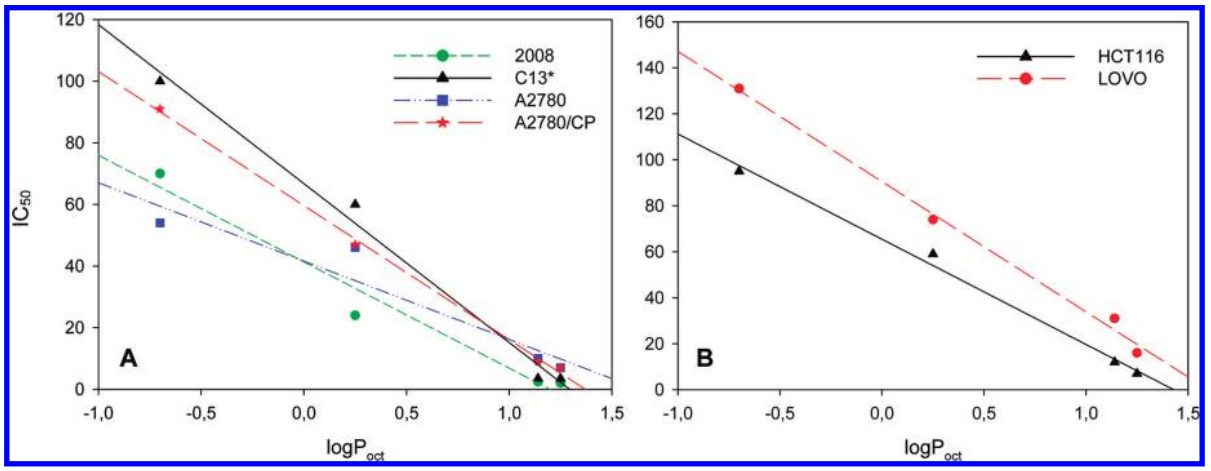

Figure 8. Correlations between IC_{50} values experimentally obtained after 48 h exposure with synthetic **A** series curcuminoids and log P_{oct} values together with linear regressions on human ovarian carcinoma cells (A) and human colon carcinoma cells (B).

concentrations slightly higher in A2780 cells, similarly to curcumin. Compounds **8** and **10** were poorly cytotoxic even at high concentrations (>100 μM).

As it concerns colon cancer cells (parts C and D of Figure 7), the **E** series is able to inhibit cell proliferation up to 70% in a lower and closer concentration range (4−5 μM in HCT116 and 6−9 μM in LoVo cells) than the **A** series compounds (>100 μM both in HCT116 and in LoVo cells), suggesting that Boc group positively affects the pharmacokinetics of these drugs, making them more lipophilic and thus facilitating their intracellular accumulation. **E** compounds are more potent inhibitors than curcumin, which requires a concentration of 4.4 μM and 20 μM on HCT116 and LoVo cell lines, respectively.

Figure 8 shows the correlation between lipophilicity, expressed by log P_{oct}, and biological activity defined as IC_{50}. For all cell lines, a linear regression is evident, showing a decrease in IC_{50} value as log P_{oct} is increased, suggesting the importance of this chemico-physical property as the driving force in cellular activity despite acidity and chemical stability, which do not show any direct relationship with cell growth inhibition.

3. CONCLUSION

The investigation here was performed to elucidate the effect on physicochemical properties of C-3 substitution in curcumin analogues highlighted interesting remarks:

(i) the insertion of alkylic chain, both in the ester and acid form, increases acidity of keto-enolic moiety and pharmacokinetic stability in physiological condition with respect to parent curcuminoid;

(ii) the alkylic chain increases molecular polarity and consequently diminishes lipophilicity with respect to curcumin, particularly for the acid series;

(iii) the C-3 substitution has no effect on radical scavenging ability with respect to the parent compounds.

Besides these general observations on C-3 substitution, which are strongly related to molecular conformations and tautomeric equililibria, the effect of aromatic substituents is instead principally connected to electronic density and resonance/inductive effects, as observed for previously investigated aromatic ring substituted curcuminoids:

(iv) among the same series, electro-withdrawing groups increase acidity of keto-enolic moiety favoring hydrophilicity and instability in physiological conditions;

(v) protic groups (phenols) are essential for the curcuminoids to exert a radical scavenging ability comparable to the parent compound.

Furthermore, our data clearly highlight an interesting antiproliferative effect for most of the synthesized compounds, suggesting that the alkyl substitution in α position of β-diketo moiety does not affect the cytotoxic activity associated with curcumin backbone. In particular, the **E** series shows IC_{50} values similar or in many cases better than curcumin in all tested cell lines and exhibits selectivity against colon carcinoma cells. Indeed, they are extremely active in HCT116 and Lovo cells after 24 h exposure at μM concentrations ca. 1/3 of curcumin: **4**, **5**, and **6** are the most effective ones. The best performances of **E** compounds with respect to **A** could be ascribed to their high lipophilicity that favors a greater and faster cellular uptake overcoming their apparently higher instability in physiological condition, however the **E** series maintains kinetic stability better than curcumin.

Interestingly, the compound **4** behaves similarly to curcumin as it concerns its free radical scavenging ability, principally due to the presence of phenolic groups on aromatic rings, and it has an increased antiproliferative activity particularly on human colon carcinoma cell lines. Even though further experiments will be needed, it is appealing to speculate that this similarity to curcumin in radical scavenging ability may lead on one side to antioxidant/protective properties in normal cells and, on the other side, may trigger apoptosis in transformed cells via enhanced ROS production.[49] Therefore the compound **4** should be considered a good candidate for future anticancer drug developments.

4. EXPERIMENTAL SECTION

4.1. General Procedures and Chemicals. Elemental analysis was performed on a CE Instruments EA 1110.

LC-MS spectra were recorded on 6310A ion trap LC-MS (Agilent Technologies) in isocratic condition (20% H_2O (0.1% HCOOH), 80% ACN) and in positive mode detection.

All chemicals were reagent grade and used without further purification unless otherwise specified. They were purchased form Sigma-Aldrich. The purity of all final compounds was determined to be at least 95% pure by a combination of HPLC, LCMS, NMR, and combustion analysis.

dx.doi.org/10.1021/jm200872q | J. Med. Chem. 2011, 54, 8066−8077

tert-Butyl 3-acetyl-4-oxopentanoate (**1**) and 3-acetyl-4-oxopentanoic acid (**2**) were synthesized as previously reported by Ferrari et al.[50]

*Preparation of E Series (**3**–**6**).* A suspension of B_2O_3 (1 mmol) and **1** (1 mmol) in DMF (1.5 mL) was stirred for 30 min at 80 °C, and then tributylborate (4 mmol) was added. After 30 min, the appropriate benzaldehyde (1.8 mmol) was added and followed by slow addition of *n*-butylamine (0.4 mmol in 0.5 mL of DMF). After stirring at 80 °C for 4 h, the solution was acidified with 0.5 M HCl (8 mL) and cooled down to room temperature. The yellow–orange solid was suspended in water, filtered, and dried under vacuum. All crude compounds were recrystallized in EtOH to give the pure products.

*(3Z-5E)-tert-Butyl-3-cinnamoyl-4-hydroxy-6-phenylhexa-3,5-dienoate (**3**).* Yellow powder, 80% yield; mp 149–150 °C. LC-MS-IT *m*/*z* 413.3 $(M + Na)^+$; 391.3 $(M + H)^+$.

KE 60%: ^{1}H NMR ($CDCl_3$) δ 3.52 (s, 2H; H-2), 7.26 (d, 2H; H-5, J = 15.2 Hz), 7.83 (d, 2H; H-6, J = 15.2 Hz), 7.64 (dd, 4H; H-8, J = 8.1 Hz, J = 1.7 Hz), 7.64 (m, 4H; H-9), 7.44 (m, 2H; H-10), 1.49 (s, 9H; $COOC(\underline{CH_3})_3$); ^{13}C NMR ($CDCl_3$) δ 170.9 (C-1), 33.5 (C-2), 105.7 (C-3), 183.6 (C-4), 120.7 (C-5), 142.0 (C-6), 135.2 (C-7), 128.2 (C-8), 128.4 (C-9), 130.1 (C-10), 81.9 ($-COO\underline{C}(CH_3)_3$), 28.3 ($-COOC(\underline{CH_3})_3$). **DK 40%**: ^{1}H NMR ($CDCl_3$) δ 3.01 (d, 2H; H-2, J = 7.3 Hz), 4.69 (t, 1H; H-3, J = 7.3 Hz), 6.91 (d, 2H; H-5, J = 15.8 Hz), 7.75 (d, 2H; H-6, J = 15.8 Hz), 7.64 (dd, 4H; H-8, J = 8.1 Hz, J = 1.7 Hz), 7.60 (m, 4H; H-9), 7.44 (m, 2H; H-10), 1.48 (s, 9H; $-COOC(\underline{CH_3})_3$); ^{13}C NMR ($CDCl_3$) δ 170.4 (C-1), 34.0 (C-2), 60.1 (C-3), 194.0 (C-4), 124.0 (C-5), 144.9 (C-6), 134.1 (C-7), 128.7 (C-8), 128.9 (C-9), 130.9 (C-10), 81.9 ($-COO\underline{C}(CH_3)_3$), 28.3 ($-COOC(\underline{CH_3})_3$).

*(3Z-5E)-tert-Butyl-4-hydroxy-6-(3-methoxy-4-hydroxyphenyl)-acrolyl)hexa3,5-dienoate (**4**).* Orange–red powder, 60% yield; mp 116.5 °C. LC-MS-IT *m*/*z* 505.2 $(M + Na)^+$; 483.3 $(M + H)^+$.

KE 50%: ^{1}H NMR (MeOD-d_4) δ 3.65 (s, 2H; H-2), 7.12 (d, 2H; H-5, J = 15.2 Hz), 7.67 (d, 2H; H-6, J = 15.2 Hz), 6.84 (d, 2H; H-8, J = 1.7 Hz), 7.17 (d, 2H; H-11, J = 8.1 Hz), 7.26 (dd, 2H; H-12, J = 1.7 Hz, J = 8.1 Hz) 3.94 (s, 6H; Ar-$OC\underline{H_3}$), 1.45 (s, 9H; $-COO(CH_3)_3$); ^{13}C NMR (MeOD-d_4) δ 172.2 (C-1), 32.6 (C-2), 105.1 (C-3), 183.2 (C-4), 117.4 (C-5), 142.2 (C-6), 127.2 (C-7), 115.2 (C-8), 148.0 (C-9), 149.8 (C-10), 123.7 (C-11), 110.6 (C-12), 55.1 (Ar–$O\underline{C}H_3$), 80.9 ($-COO\underline{C}(CH_3)_3$), 26.8 ($-C(\underline{C}H_3)_3$). **DK 50%**: ^{1}H NMR (MeOD-d_4) δ 2.90 (s, 2H; H-2), 6.93 (d, 2H; H-5, J = 15.9 Hz), 7.70 (d, 2H; H-6, J = 15.9 Hz), 6.86 (d, 2H; H-8, J = 1.7 Hz), 7.17 (d, 2H; H-11, J = 8.1 Hz), 7.26 (dd, 2H; H-12, J = 1.7 Hz, J = 8.1 Hz), 3.87 (s, 6H; Ar-$OC\underline{H_3}$), 1.44 (s, 9H; $-COO(C\underline{H_3})_3$); ^{13}C NMR (MeOD-d_4) δ 171.0 (C-1), 33.7 (C-2), 58.0 (C-3), 194.8 (C-4), 121.5 (C-5), 145.3 (C-6), 126.2 (C-7), 115.2 (C-8), 148.0 (C-9), 149.8 (C-10), 123.7 (C-11), 110.6 (C-12), 55.0 (Ar–$O\underline{C}H_3$), 80.9 ($-\underline{C}(CH_3)_3$), 26.8 ($-C(\underline{C}H_3)_3$).

*(3Z-5E)-tert-Butyl-4-hydroxy-6-(3-methoxyphenyl)acrolyl)-hexa3,5-dienoate (**5**).* Dark-yellow powder, 60% yield; mp 152–153 °C. LC-MS-IT *m*/*z* 473.2 $(M + Na)^+$; 451.3 $(M + H)^+$.

KE 52%: ^{1}H NMR ($CDCl_3$) δ 3.51 (s, 2H; H-2), 7.22 (d, 2H; H-5, J = 15.3 Hz), 7.78 (d, 2H; H-6, J = 15.3 Hz), 7.15 (d, 2H; H-8, J = 1.9 Hz), 6.98 (m, 2H; H-10), 7.36 (t, 2H; H-11, J = 8.2 Hz), 7.25 (dd, 2H; H-12, J = 1.9 Hz, J = 8.2 H), 3.90 (s, 6H; Ar–$O\underline{CH_3}$), 1.48 (s, 9H; $-C(C\underline{H_3})_3$); ^{13}C NMR ($CDCl_3$) δ 170.87 (C-1), 33.5 (C-2), 105.8 (C-3), 183.5 (C-4), 121.0 (C-5), 141.9 (C-6), 136.9 (C-7), 113.4 (C-8), 159.8 (C-9), 115.7 (C-10), 129.8 (C-11), 120.7 (C-12), 55.4 (Ar–$O\underline{C}H_3$), 81.5 ($-\underline{C}(CH_3)_3$), 28.0 ($-C(\underline{C}H_3)_3$). **DK 48%**: ^{1}H NMR ($CDCl_3$) δ 3.01 (d, 2H; H-2, J = 7.2 Hz), 4.69 (t, 1H; H-3, J = 7.2 Hz), 6.88 (d, 2H; H-5, J = 15.9 Hz), 7.71 (d, 2H; H-6, J = 15.9 Hz), 7.10 (d, 2H; H-8, J = 1.9 Hz), 6.98 (m, 2H; H-10), 7.36 (t, 2H; H-11, J = 8.2 Hz), 7.25 (dd, 2H; H-12, J = 1.9 Hz, J = 8.2 H), 3.86 (s, 6H; Ar-$OC\underline{H_3}$), 1.48 (s, 9H; $COOC(C\underline{H_3})_3$); ^{13}C NMR ($CDCl_3$) δ 170.3 (C-1), 34.0 (C-2), 60.0 (C-3), 193.8 (C-4), 124.2 (C-5), 144.8 (C-6), 136.9 (C-7), 113.2 (C-8), 159.9 (C-9), 115.7 (C-10), 129.8 (C-11), 120.7 (C-12), 55.4 (Ar–$O\underline{C}H_3$), 81.4 ($-COO\underline{C}(CH_3)_3$), 27.9 ($-COOC(\underline{CH_3})_3$).

*4,4′-((1E,3Z,6E)-4-(2-tert-Butoxy-2-oxoethyl)-3-hydroxy-5-oxo-hepta-1,3,6-triene-1,7-diyl)bis(2-methoxy-4,1-phenylene)diacetate (**6**).* Yellow powder, 47% yield; mp 152–153 °C. LC-MS-IT *m*/*z* 567.3 $(M + Na)^+$; 589.3 $(M + H)^+$.

KE 43%: ^{1}H NMR ($CDCl_3$) δ 3.50 (s, 2H; H-2), 7.16 (d, 2H; H-5, J = 15.2 Hz), 7.77 (d, 2H; H-6, J = 15.2 Hz), 7.19 (d, 2H; H-8, J = 1.7 Hz), 7.25 (d, 2H; H-11, J = 8.1 Hz), 7.11 (dd, 2H; H-12, J = 1.7 Hz, J = 8.1 Hz), 3.89 (s, 6H; Ar-$OC\underline{H_3}$), 2.36 (s, 6H; Ar–$O(CO)C\underline{H_3}$), 1.47 (s, 9H, $-COOC(C\underline{H_3})_3$); ^{13}C NMR ($CDCl_3$) δ 170.7 (C-1), 33.5 (C-2), 105.6 (C-3), 183.4 (C-4), 120.9 (C-5), 141.5 (C-6), 134.2 (C-7), 111.9 (C-8), 151.4 (C-9), 141.9 (C-10), 121.0 (C-11), 123.21 (C-12), 56.0 (Ar–$O\underline{C}H_3$), 20.6 (Ar–$O(CO)\underline{C}H_3$), 81.4 ($-COO\underline{C}-(CH_3)_3$), 28.1 ($-COOC(\underline{C}H_3)_3$), 168.7 (Ar–$O(\underline{C}O)CH_3$). **DK 57%**: ^{1}H NMR ($CDCl_3$) δ 3.01 (d, 2H; H-2, J = 7.1 Hz), 4.67 (t, 1H; H.3, J = 7.1 Hz), 6.83 (d, 2H; H-5, J = 15.8 Hz), 7.69 (d, 2H; H-6, J = 15.8 Hz), 7.15 (d, 2H; H-8, J = 1.7 Hz), 7.25 (d, 2H; H-11, J = 8.1 Hz), 7.11 (dd, 2H; H-12, J = 1.7 Hz, J = 8.1 Hz), 3.93 (s, 6H; Ar-$OC\underline{H_3}$), 2.37 (s, 6H; Ar–$O(CO)C\underline{H_3}$), 1.47 (s, 9H; $COOC(C\underline{H_3})_3$); ^{13}C NMR ($CDCl_3$) δ 170.3 (C-1), 33.9 (C-2), 60.1 (C-3), 193.7 (C-4), 124.0 (C-5), 144.2 (C-6), 133.0 (C-7), 111.6 (C-8), 151.4 (C-9), 141.9(C-10), 120.9 (C-11), 122.0 (C-12), 56.0 (Ar–$O\underline{C}H_3$), 20.6 (Ar–$O(CO)\underline{C}H_3$), 81.4 ($-COO\underline{C}(CH_3)_3$), 28.1 ($-COOC(\underline{C}H_3)_3$), 168.7 (Ar–$O(\underline{C}O)CH_3$).

*Preparation of A Series (**7**–**10**). Route **a**.* The removal of the Boc group from **E** compounds gives **A** series. The reaction was accomplished by addition TFA (50% in CH_2Cl_2) under continuous stirring for 1 h at 0 °C.[51] The organic phase was washed three times with distilled water, and then dried under Na_2SO_4, concentrated, and purified through flash column chromatography (silica gel, mesh 0.035–0.070 mm, mobile phase: *n*-hexane/EtOAc 5/5).

*Route **b**.* A suspension of B_2O_3 (2.25 mmol) and 2 (3.0 mmol) in DMF (4 mL) was stirred for 30 min at 70 °C. A solution of the appropriate benzaldehyde (6.0 mmol), AcOH (1,1 mL), and morpholine (0.60 mmol) in DMF (4 mL) was added. The stirring continued for 5 h at 70 °C. The mixture was then hydrolyzed at room temperature by adding an aqueous solution 20% AcOH (36 mL) and stirring 1 h. The mixture was then extracted twice with EtOAc. The combined organic layers were washed with brine and water until neutral pH, dried over Na_2SO_4, and evaporated under reduced pressure to afford an oil, which was purified by flash column chromatography. Silicagel, mesh 0.035–0.070 mm, mobile phase referred to compound **8**: petroleum ether/EtOAc/AcOH 70/30/0.3.

*(3Z-5E)-3-Cinnamoyl-4-hydroxy-6-phenylhexa-3,5-dienoic Acid (**7**).* Pale-yellow powder, yield: 67% (route ***a***); mp 163–164 °C. LC-MS-IT *m*/*z* 357.2 $(M + Na)^+$; 335.3 $(M + H)^+$. **KE 48%**: ^{1}H NMR (MeOD-d_4) δ 3.72 (s, 2H; H-2), 7.29 (d, 2H; H-5, J = 15.2 Hz), 7.76 (d, 2H; H-6, J = 15.2 Hz), 7.67 (dd, 4H; H-8, J = 1.8 Hz,, J = 8.2 Hz), 7.67 (m, 4H; H-9), 7.43 (m, 2H; H-10); ^{13}C NMR (MeOD-d_4) δ 174.4 (C-1), 30.8 (C-2), 105.5 (C-3), 183.0 (C-4), 120.3 (C-5), 141.9 (C-6), 134.1 (C-7), 130.9 (C-10), 128.4 (C-11), 127.9 (C-12). **DK 52%**: ^{1}H NMR (MeOD-d_4) δ 3.00 (s, 2H; H-2), 7.08 (d, 2H; H-5, J = 15.8 Hz), 7.77 (d, 2H; H-6, J = 15.8 Hz), 7.67 (dd, 4H; H-8, J = 1.8 Hz, J = 8.2 Hz), 7.67 (m, 4H; H-9), 7.43 (m, 2H; H-10); ^{13}C NMR (MeOD-d_4) δ 173.3 (C-1), 32.0 (C-2), 57.9 (C-3), 194.7 (C-4), 124.5 (C-5), 144.6 (C-6), 135.2 (C-7), 128.1 (C-8), 128.4 (C-9), 130.9 (C-10).

*(3Z,5E)-6-(3-Methoxy-4-hydroxyphenyl)-3-((E)-3-(3-methoxy-4-hydroxyphenyl)acryloyl)-4-hydroxyhexa-3,5-dienoic Acid (**8**).* Orange–red powder, yield: 21% (route ***b***); mp 158–159 °C. LC-MS-IT *m*/*z* 449.1 $(M + Na)^+$; 427.1 $(M + H)^+$.

KE 25%: ^{1}H NMR (MeOD-d_4) δ 3.68 (s, 2H, H-2), 7.08 (d, 2H, H-5, J = 15.1 Hz), 7.66 (d,2H, H-6, J = 15.1 Hz), 7.24 (d, 2H, H-8, J = 1.6 Hz), 6.82 (d, 2H, H-11, J = 8.2 Hz), 7.13 (dd, 2H, H-12, J = 1.6 Hz, J = 8.2 Hz), 3.91 (s, 6H, Ar-$OC\underline{H_3}$); ^{13}C NMR (MeOD-d_4) δ 176.4 (C-1), 32.7 (C-2), 106.5 (C-3), 184.8 (C-4), 118.8 (C-5), 143.6 (C-6), 128.9 (C-7), 112.0 (C-8), 149.4 (C-9), 150.5 (C-10), 116.6 (C-11), 124.3 (C-12), 56.5 (Ar–$O\underline{C}H_3$). **DK 75%**: ^{1}H NMR (MeOD-d_4) δ 2.96 (s, 2H, H-2), 6.91 (d, 2H, H-5, J = 15.9 Hz), 7.68 (d, 2H, H-6, J = 15.9 Hz), 7.22 (d, 2H, H-8 J = 1.6 Hz), 6.81 (d, 2H, H-11, J = 8.2 Hz), 7.14 (dd, 2H, H-12, J = 1.6 Hz, J = 8.2 Hz), 3.85 (s, 6H, Ar-$OC\underline{H_3}$); ^{13}C NMR (MeOD-d_4) δ 175.1 (C-1), 33.7 (C-2), 59.4 (C-3), 196.2 (C-4), 123.1 (C-5), 146.8 (C-6), 127.6 (C-7), 112.0 (C-8),

dx.doi.org/10.1021/jm200872q | *J. Med. Chem.* 2011, 54, 8066–8077

149.5 (C-9), 151.4 (C-10), 116.6 (C-11), 125.2 (C-12), 56.4 (Ar−O$\underline{C}H_3$).

*(3Z-5E)-4-Hydroxy-6-(3-methoxyphenyl)acrolyl)hexa3,5-dienoic Acid (**9**).* Orange−yellow powder, yield: 62% (route ***a***); mp 191−192 °C. LC-MS-IT m/z 417.2 $(M + Na)^+$; 395.2 $(M + H)^+$. **KE 43%**: ^{1}H NMR (MeOD-d_4) δ 3.70 (s, 2H; H-2), 7.28 (d, 2H; H-5, J = 15.3 Hz), 7.72 (d, 2H; H-6, J = 15.3 Hz), 7.22 (d, 2H, H-8, J = 1.9 Hz), 7.00 (dd, 2H, H-10, J = 1.9 Hz, J = 8.2 Hz), 7.34 (t, 2H, H-11, J = 8.2 Hz), 7.24 (dd, 2H, H-12, J = 1.9 Hz, J = 8.2 Hz), 3.86 (Ar-O$\underline{C}H_3$); ^{13}C NMR (MeOD-d_4) δ 174.9 (C-1), 31.6 (C-2), 106.1 (C-3), 183.1 (C-4), 120.8 (C-5), 141.6 (C-6), 160.1 (C-9), 54.5 (Ar−O$\underline{C}H_3$). **DK 57%**: ^{1}H NMR (MeOD-d_4) δ 2.98 (s, 2H, H-2), 7.08 (d, 2H, H-5, J = 15.9 Hz), 7.73 (d, 2H, H-6, J = 15.9 Hz), 7.22 (d, 2H, H-8, J = 1.9 Hz), 7.00 (dd, 2H, H-10, J = 1.9 Hz, J = 8.2 Hz), 7.34 (t, 2H, H-11, J = 8.2 Hz), 7.24 (dd, 2H, H-12, J = 1.9 Hz, J = 8.2 Hz), 3.82 (Ar-O$\underline{C}H_3$); ^{13}C NMR (MeOD-d_4) δ 173.8 (C-1), 32.4 (C-2), 57.6 (C-3), 194.8 (C-4), 124.9 (C-5), 144.5 (C-6), 136.5 (C-7), 112.6 (C-8), 160.1 (C-9), 116.7 (C-10), 129.8 (C-11), 120.2 (C-12), 54.1 (Ar−O$\underline{C}H_3$).

*(3Z,5E)-6-(4-Acetoxy-3-methoxyphenyl)-3-((E)-3-(4-acetoxy-3-methoxyphenyl)acryloyl)-4-hydroxyhexa-3,5-dienoic Acid (**10**).* Orange−yellow powder, yield: 60% (route ***a***); mp 130−131 °C. LC-MS-IT m/z 533.2 $(M + Na)^+$; 511.2 $(M + H)^+$. **KE 30%**: ^{1}H NMR (MeOD-d_4) δ 3.76 (s, 2H, H-2), 6.96 (d, 2H, H-5, J = 15.2 Hz), 7.73 (d, 2H, H-6, J = 15.2 Hz), 7.39 (d, 2H, H-8, J = 1.7 Hz), 7.28 (d, 2H, H-11, J = 8.1 Hz), 7.10 (dd, 2H, H-12, J = 1.7 Hz, J = 8.1 Hz), 2.29 (Ar−O(CO)C$\underline{H}_3$), 3.90 (Ar−OC$\underline{H}_3$); ^{13}C NMR (MeOD-d_4) δ 174.6 (C-1), 31.2 (C-2), 106.7 (C-3), 183.2 (C-4), 115.2 (C-5), 141.1 (C-6), 134.3 (C-7), 111.4 (C-8), 151.6 (C-9), 141.9 (C-10), 121.1 (C-11), 122.9 (C-12), 55.1 (Ar−O$\underline{C}H_3$), 19.0 (Ar−O(CO)$\underline{C}H_3$), 169.0 (Ar−O($\underline{C}$O)CH$_3$). **DK 70%**: ^{1}H NMR (MeOD-d_4) δ 3.01 (s, 2H, H-2), 7.09 (d, 2H, H-5, J = 15.8 Hz), 7.75 (d, 2H, H-6, J = 15.8 Hz), 7.37 (d, 2H, H-8, J = 1.7 Hz), 7.28 (d, 2H, H-11, J = 8.1 Hz), 7.10 (dd, 2H, H-12, J = 1.7 Hz, J = 8.1 Hz), 2.28 (Ar−O(CO)C$\underline{H}_3$), 3.84 (Ar−OC$\underline{H}_3$). ^{13}C NMR (MeOD-d_4) δ 173.5 (C-1), 32.2 (C-2), 58.1 (C-3), 194.7 (C-4), 124.9 (C-5), 143.7 (C-6), 133.3 (C-7), 111.4 (C-8), 151.6 (C-9), 141.9 (C-10), 121.1 (C-11), 122.9 (C-12),55.1 (Ar−O$\underline{C}H_3$), 19.0 (Ar−O(CO)$\underline{C}H_3$), 169.0 (Ar−O($\underline{C}$O)CH$_3$).

4.2. Crystal Data. The diffraction data were collected at room temperature with Bruker-Nonius X8APEX single-crystal diffractometer controlled by Bruker-Nonius X8APEX software using Mo Kα radiation (λ = 0.71073 Å). The structure was solved by direct method and refined by full-matrix, lest-squares procedures (based on F_o^2) using WINGX system of crystallographic computer programs.[52] All non-hydrogen atoms were refined anisotropically, and hydrogen atoms were located in a Fourier map and refined isotropically. The crystal data and refinement parameters are summarized in Table 6.

4.3. Spectroscopy. Spectrophotometric measurements were performed using Jasco V-570 spectrophotometer at 25 ± 0.1 °C in the 200−600 nm spectral range employing 1 cm quartz cells. pH-Metric titrations were obtained varying the pH value by adding small amounts of concentrated NaOH or HCl in the pH range 1−11. A constant ionic strength of 0.1 M ($NaNO_3$) was maintained in all experiments. The overall stability constants (expressed as log β_{LH}) and pK_a values were evaluated from spectrophotometric data using the software pHab.[36]

NMR spectra were recorded on a Bruker Avance AMX-400 spectrometer with a Broad Band 5 mm probe (inverse detection). Nominal frequencies were 100.13 MHz for ^{13}C and 400.13 MHz for ^{1}H. The typical acquisition parameters for ^{1}H were as follows: 20 ppm spectral bandwidth (SW), 6.1 μs pulse width (90° hard pulse on ^{1}H), 0.5−1 s pulse delay, 216−512 number of scans. For 2D H,H-homonuclear correlated spectroscopy (COSY), typical parameters were used. For 2D H,X-hetero correlated spectroscopy, HMBC and HMQC opportune parameters were used (50−90° pulses; 32 k data points; 1 s relaxation delay; 8−64 k transients; $^1J_{H-C}$ 125−145 Hz; $^3J_{H-C}$ 5−15 Hz). CD_3OD-d_4, DMSO-d_6, and $CDCl_3$ were used as NMR solvent. All reported chemical shifts (δ) are expressed in ppm and are referred to TMS.

4.4. Kinetic Stability. The chemical stability at 37 °C in darkness of both **T** and **A** series was evaluated by UV−vis spectroscopy as a change in absorbance in the 200−600 nm range over an overall period of 8 h. Then 50 μM solutions of the ligands were prepared in 0.1 M TRIS-HCl buffer (pH 7.4). A constant ionic strength of 0.1 M ($NaNO_3$) was maintained in all experiments. Spectra were recorded every 30 min. All profiles were linearized by an hyperbolic function (eq 1), which represents an empirical model that well describes drug decomposition or release.[37]

$$\frac{t}{f_{\%}} = at + b \qquad (1)$$

where $f_{\%}$ is the fraction of residual compound at time t (min) expressed as percentage referred to starting concentration at *time zero*.

4.5. Solubility. The appropriate amount of each **A** compound was shaken with a known volume of buffered aqueous solution (0.1 M TRIS-HCl, pH = 7.4) at room temperature for 30 min in order to provide a saturated solution with a precipitate. The supernatant was filtered through a 0.2 μm disposable membrane filter (OlimPeak, Tekno Kroma), and the concentration of ligand in the resultant solution was determined (after an appropriate dilution) by UV−vis spectroscopy.

4.6. Partition Coefficient. The shaken-flask method was performed in buffered condition (TRIS-HCl pH 7.4). Ten mL stock solutions of each compound (50 μM) were mixed in a vessel with known volumes of high purity analytical grade *n*-octanol (2, 4, 6, 8, 10 mL) and shaken at 37 °C for 2 h. After separating the two phases, the ligand concentration in the aqueous solution was determined by UV−vis spectroscopy by reading absorbance at λ = 300 nm.

4.7. Antioxidant Activity (DPPH Radical Scavenging Method). The antioxidant activity of curcuminoids was determined in terms of hydrogen donating or radical scavenging ability, using the stable radical DPPH. A variable amount (15, 30, 45, 75, 105, and 150 μL) of a methanolic solution (1.2 mM) of each compound, including curcumin as benchmark, was placed in a cuvette, and 3 mL of a 6×10^{-5} M methanolic solution of DPPH was added. Absorbance measurements initiated immediately. The decrease in absorbance at 517 nm was determined continuously every minute up to 5 min, then every 5 min up to 30 min and every 30 min until reaction reaches completeness and absorbance stabilizes attaining a plateau after

Table 6. Crystal Data and Structure Refinement for Compound 5

empirical formula	C_{27} H_{30} O_6
formula wt	450.51
temp	293(2) K
wavelength	0.71073 Å
crystal system, space group	triclinic $P\bar{1}$
unit cell dimensions	a = 10.3080(10) Å α = 63.957(4)°
	b = 10.9062(9) Å β = 82.789(3)°
	c = 12.1041(9) Å γ = 86.318(3)°
vol	1212.86(18) Å^3
Z, calcd density	2, 1.234 g/cm^3
absorption coefficient	0.086 mm^{-1}
F(000)	480
crystal size	0.3 × 0.2 × 0.3 mm
θ range for data collection	3.77−19.19°
limiting indices	$-9 \le h \le 9$, $-9 \le k \le 10$, $-11 \le l \le 10$
reflns collected/unique	5076/1946 [R(int) = 0.0449]
completeness to θ = 19.19	96.6%
absorption correction	none
refinement method	full-matrix least-squares on F^2
data/restraints/parameters	1946/0/389
goodness-of-fit on F^2	0.800
final R indices [I > 2σ (I)]	R_1 = 0.0399, wR_2 = 0.0943
R indices (all data)	R_1 = 0.0761, wR_2 = 0.1167
extinction coefficient	0.0000(12)
largest diff. peak and hole	0.106 and −0.103 e·Å^{-1}

dx.doi.org/10.1021/jm200872q | J. Med. Chem. 2011, 54, 8066−8077

120 min. Methanol was used to zero the spectrophotometer. The absorbance of the DPPH radical without antioxidant, i.e. the control, was measured daily, and concentration was calculated applying eq 2:[53]

$$[\mathrm{DPPH}^{\bullet}] = \frac{A - 1.006}{10970} \quad (2)$$

The percentage of inhibition (%In) of the DPPH radical by each sample was calculated according to the formula:

$$\%\mathrm{In} = \frac{A_0 - A_t}{A_0} \times 100 \quad (3)$$

where A_0 represents the absorbance of the control (DPPH radical) at time 0, while A_t refers to the absorbance of the mixture DPPH/antioxidant at time t (120 min). Values of absorbance were corrected taking into account volume dilution and all determinations were performed in triplicate.

4.8. Cell Lines. The 2008 cell line was established from a patient with serous cystadenocarcinoma of the ovary, and the cDDP-resistant C13* subline, about 15-fold resistant to cDDP, was derived from the parent 2008 cell line by monthly exposure to cDDP, followed by chronic exposure to stepwise increases in cDDP concentration.[47] The human ovarian carcinoma A2780/CP cells are 12-fold resistant to cDDP and derived from the parent A2780 cell line. These human ovarian cell lines were grown as monolayers in RPMI 1640 medium containing 10% heat-inactivated fetal bovine serum and 50 μg/mL gentamycin sulfate. All cell media and serum were purchased from Lonza, Verviers, Belgium. Cultures were equilibrated with humidified 5% CO_2 in air at 37 °C. All studies were performed in *Mycoplasma* negative cells, as routinely determined with the Mycotest detection kit (Euroclone, Switzerland).

Human colon carcinoma HCT116 cells were generously provided by Bert Volgestein (Johns Hopkins University School of Medicine, Baltimore, MD, USA). The cells were cultured in Iscoves' modified Dulbecco medium (IMDM) containing 10% fetal bovine serum (Euroclone), 2 mM glutamine, 100 IU/mL penicillin, and 100 mg/mL streptomycin at 37 °C and in presence of 5% CO_2. Human adenocarcinoma LoVo cell line was cultured in Dulbecco's Modified Medium (DMEM).

4.9. Cell Growth Assay. To define IC_{50} values, drugs were added to warm cell medium at the concentration and time exposure described in the text. Cell growth was determined by a modification of the crystal violet dye assay.[54] On selected days, after removal of the cell culture medium, the cell monolayer was fixed with methanol prior to staining with 0.05% crystal violet solution in 20% methanol for at least 30 min. After washing several times with distilled water to remove the dye excess, the cells were allowed to dry. The incorporated dye was solubilized in acidic isopropanol (1N HCl: 2-propanol, 1:10) and determined spectrophotometrically at 540 nm by a Tecan GENios Pro (Tecan Trading AG, Switzerland) plate reader. The extracted dye was proportional to cell number. Percentage of cytotoxicity was calculated by comparing the absorbance of exposed to nonexposed (control) cultures.

■ ASSOCIATED CONTENT

Ⓢ Supporting Information

Additional experimental details (elemental analysis for compounds **3**−**10** and crystal data for **5**). This material is available free of charge via the Internet at http://pubs.acs.org. Crystallographic data (excluding structure factors) have been deposited with the Cambridge Crystallographic Data Center as Supplementary Publication no. CCDC 838903. Copies of the data can be obtained free for charge on application to CCDC, 12 Union Road, Cambridge CB2 1EZ, U.K. [fax +44 1223−336−033; e-mail deposit@ccdc.cam.ac.uK].

■ AUTHOR INFORMATION

Corresponding Author

*Phone: +39 059 2055040. Fax: +39 059373543. E-mail: monica.saladini@unimore.it.

■ ACKNOWLEDGMENTS

We are grateful to the "Centro Interdipartimentale Grandi Strumenti−CIGS" of the University of Modena and Reggio Emilia for supplying advanced instrumentations and skilled technicians. This work was supported by Associazione Italiana per la Ricerca sul Cancro-MFAG to CI (grant no. 6192).

■ REFERENCES

(1) Teiten, M.-H.; Eifes, S.; Dicato, M.; Diederich, M. Curcumin-The Paradigm of a Multi-Target Natural Compound with Applications in Cancer Prevention and Treatment. *Toxins* **2010**, *2*, 128−162.

(2) Anand, P.; Sundaram, C.; Jhurani, S.; Kunnumakkara, A. B.; Aggarwal, B. B. Curcumin and cancer: an "old-age" disease with an "age-old" solution. *Cancer Lett.* **2008**, *267*, 133−164.

(3) Sa, G.; Das, T. Anti cancer effects of curcumin: cycle of life and death. *Cell Div.* **2008**, *3*, 1−14.

(4) Shehzad, A.; Wahid, F.; Lee, Y. S. Curcumin in Cancer Chemoprevention: Molecular Targets, Pharmacokinetics, Bioavailability and Clinical Trials. *Arch. Pharm. Chem. Life Sci.* **2010**, *343*, 489−499.

(5) Patel, B. B.; Majumdar, A. P. Synergistic role of Curcumin with current therapeutics in colorectal cancer: minireview. *Nutr Cancer* **2009**, *61*, 842−846.

(6) Milacic, V.; Banerjee, S.; Landis-Piwowar, K. R.; Sarkar, F. H.; Majumdar, A. P.; Dou., Q. P. Curcumin inhibits the proteasome activity in human colon cancer cells in vitro and in vivo. *Cancer Res.* **2008**, *68*, 7283−7292.

(7) Basile, V.; Ferrari, E.; Lazzari, S.; Belluti, S.; Pignedoli, F.; Imbriano, C. Curcumin derivatives: molecular basis of their anti-cancer activity. *Biochem. Pharmacol.* **2009**, *78*, 1305−1315.

(8) Watson, J. L.; Hill, R.; Lee, P. W.; Giacomantonio, C. A.; Hoskin, D. W. Curcumin induces apoptosis in HCT-116 human colon cancer cells in a p21-independent manner. *Exp. Mol. Pathol.* **2008**, *84*, 230−233.

(9) Chen, H.; Zhang, Z. S.; Zhang, Y. L.; Zhou, D. Y. Curcumin inhibits cell proliferation by interfering with the cell cycle and inducing apoptosis in colon carcinoma cells. *Anticancer Res.* **1999**, *19*, 3675−3680.

(10) Watson, J. L.; Greenshields, A.; Hill, R.; Hilchie, A.; Lee, P. W.; Giacomantonio, C. A.; Hoskin, D. W. Curcumin-induced apoptosis in ovarian carcinoma cells is p53-independent and involves p38 mitogen-activated protein kinase activation and downregulation of Bcl-2 and survivin expression and Akt signaling. *Mol. Carcinog.* **2010**, *49*, 13−24.

(11) Montopoli, M.; Ragazzi, E.; Froldi, G.; Caparrotta, L. Cell-cycle inhibition and apoptosis induced by curcumin and cisplatin or oxaliplatin in human ovarian carcinoma cells. *Cell Prolif.* **2009**, *42*, 195−206.

(12) Ferrari, E.; Lazzari, S.; Marverti, G.; Pignedoli, F.; Spagnolo, F.; Saladini, M. Synthesis, cytotoxic and combined cDDP activity of new stable curcumin derivatives. *Bioorg. Med. Chem.* **2009**, *17*, 3043−3052.

(13) Kelland, L. R.; Kimbell, R.; Hardcastle, A.; Aherne, G. W.; Jackman, A. L. Relationship between resistance to Cisplatin and antifolates in sensitive and resistant tumour cell lines. *Eur. J. Cancer* **1995**, *31A*, 981−986.

(14) Aggarwal, B. B.; Kumar, A.; Bharti, A. C. Anticancer potential of curcumin: preclinical and clinical studies. *Anticancer Res.* **2003**, *23*, 363−398.

(15) Wang, Y. J.; Pan, M. H.; Cheng, A. L.; Lin, L. I.; Ho, Y. S.; Hsieh, C. Y.; Lin, J. K. Stability of curcumin in buffer solutions and characterization of its degradation products. *J. Pharm. Biomed. Anal.* **1997**, *15*, 1867−1876.

(16) Tønnesen, H. H.; Másson, M.; Loftsson, T. Studies of curcumin and curcuminoids. XXVII. Cyclodextrin complexation: solubility, chemical and photochemical stability. *Int. J. Pharm.* **2002**, *244*, 127−135.

(17) Lopez-Lazaro, M. Anticancer and carcinogenic properties of curcumin: considerations for its clinical development as a cancer chemopreventive and chemotherapeutic agent. *Mol. Nutr. Food Res.* **2008**, *52*, S103−S127.

(18) Syng-Ai, C.; Kumari, A. L.; Khar, A. Effect of curcumin on normal and tumor cells: role of glutathione and bcl-2. *Mol. Cancer Ther.* **2004**, *3*, 1101−1108.
(19) Aggarwal, B. B.; Surh, Y.-Y.; Shishodia, S. Advances in Experimental Medicine and Biology Vol. *595* "The Molecular Targets and Therapeutic Uses of Curcumin in Health and Disease 2007, Springer.
(20) Huang, Q.; Yu, H.; Ru, Q. Bioavailability and Delivery of Nutraceuticals Using Nanotechnology. *J. Food Sci.* **2010**, *75*, R50−R57.
(21) Kumar, S.; Narain, U.; Tripathi, S.; Misra, K. Syntheses of Curcumin Bioconjugates and Study of Their Antibacterial Activities against β-Lactamase-Producing Microorganisms. *Bioconjugate Chem.* **2001**, *12*, 464−469.
(22) Safavy, A.; Raisch, K. P.; Mantena, S.; Sanford, L. L.; Sham, S. W.; Rama Krishna, N.; Bonner, J. A. Design and Development of Water-Soluble Curcumin Conjugates as Potential Anticancer Agents. *J. Med. Chem.* **2007**, *50*, 6284−6288.
(23) Yen, F.-L.; Wu, T.-H.; Tzeng, C.-W.; Lin, L.-T.; Lin, C.-C. Curcumin Nanoparticles Improve the Physicochemical Properties of Curcumin and Effectively Enhance Its Antioxidant and Antihepatoma Activities. *J. Agric. Food Chem.* **2010**, *58*, 7376−7382.
(24) Shoba, G.; Joy, D.; Joseph, T.; Majeed, M.; Rajendran, R.; Srinivas, P. S. Influence of piperine on the pharmacokinetics of curcumin in animals and human volunteers. *Planta Med.* **1998**, *64*, 353−356.
(25) Ohori, H.; Yamakoshi, H.; Tomizawa, M.; Shibuya, M.; Kakudo, Y.; Takahashi, A.; Takahashi, S.; Kato, S.; Suzuki, T.; Ishioka, C.; Iwabuchi, Y.; Shibata, H. Structure−activity relationship studies of curcumin analogues. *Mol. Cancer Ther.* **2006**, *5*, 2563−2571.
(26) Ohtsu, H.; Xiao, Z.; Ishida, J.; Nagai, M.; Wang, H. K.; Itokawa, H.; Su, C. Y.; Shih, C.; Chiang, T.; Chang, E.; Lee, Y.; Tsai, M. Y.; Chang, C.; Lee, K. H. Antitumor Agents. 217. Curcumin Analogues as Novel Androgen Receptor Antagonists with Potential as Anti-Prostate Cancer Agents. *J. Med. Chem.* **2002**, *45*, 5037−5042.
(27) Pabon, H. J. J. A synthesis of curcumin and related compounds Rec. Trav. Chim. Pays-Bas 1964; *83*; 379-386.
(28) Lin, L.; Shi, Q.; Nyarko, A. K.; Bastow, K. F.; Wu, C.-C.; Su, C.-Y.; Shih, C.C-Y.; Lee, K.-H. Antitumor Agents. 250.† Design and Synthesis of New Curcumin Analogues as Potential Anti-Prostate Cancer Agents. *J. Med. Chem.* **2006**, *49*, 3963−3972.
(29) Lin, L.; Shi, Q.; Su, C.-Y.; Shih, C.C-Y.; Lee, K.-H. Antitumor agents 247. New 4-ethoxycarbonylethyl curcumin analogs as potential antiandrogenic agents. *Bioorg. Med. Chem.* **2006**, *14*, 2527−2534.
(30) Babu, K. V. D.; Rajasekharan, K. N. Simplified condition for synthesis of curcumin I and other curcuminoids. *Org. Prep. Proc. Int.* **1994**, *26*, 674−677.
(31) Brunett, M. N.; Johnson, C. K. ORTEP III, Report ORNL-6895, Oak Ridge National Laboratory, Tennessee, USA, 1996.
(32) Emsley, J. The composition, structure and hydrogen bonding of the β-diketones *Struct. Bonding (Berlin)* (Berlin), 1984, *57*, 147−191.
(33) Tønnesen, H. H.; Karlsen, J.; Mostad, A. Structural Studies of Curcuminoids. I. The Crystal Structure of Curcumin. *Acta Chem. Scand. B* **1982**, *B36*, 475−479.
(34) Bertolasi, V.; Ferretti, V.; Gilli, P.; Yao, C. L. Substituent effects on keto−enol tautomerization of β-diketones from X-ray structural data and DFT calculations. *New J. Chem.* **2008**, *32*, 694−704.
(35) Caselli, M.; Ferrari, E.; Imbriano, C.; Pignedoli, F.; Saladini, M.; Ponterini, G. Probing solute−solvent hydrogen bonding with fluorescent water-soluble curcuminoids. *J. Photochem. Photobiol. A: Chem.* **2010**, *210*, 115−124.
(36) Gans, P.; Sabatini, A.; Vacca, A. Determination of equilibrium constants from spectrophotometric data obtained from solutions of known pH: the program pHab. *Ann. Chim.* **1999**, *89*, 45−49.
(37) Arcos, D.; Lopez-Noriega, A.; Ruiz-Hernandez, E.; Terasaki, O.; Vallet-Regí, M. Ordered Mesoporous Microspheres for Bone Grafting and Drug Delivery. *Chem. Mater.* **2009**, *21*, 1000−1009.
(38) Lipinski, C. A.; Lombardo, F.; Dominy, B. W.; Feeney, P. J. Experimental and computational approaches to estimate solubility and permeability in drug discovery and development settings. *Adv. Drug Delivery Rev.* **2001**, *46*, 3−26.
(39) Toulmin, A.; Wood, J. M.; Kenny, P. W. Toward Prediction of Alkane/Water Partition Coefficients. *J. Med. Chem.* **2008**, *51*, 3720−3730.
(40) Liu, Z. D.; Hider, R. C. Design of clinically useful iron(III)-selective chelators. *Med. Res. Rev.* **2002**, *22*, 26−64.
(41) Ak, T.; Gülçin, İ. Antioxidant and radical scavenging properties of curcumin. *Chem. Biol. Interact.* **2008**, *174*, 27−37.
(42) Priyadarsini, K. I.; Maity, D. K.; Naik, G. H.; Sudheer Kumar, M.; Unnikrishnan, M. K.; Satav, J. G.; Mohan, H. *Free Radical Biol. Med.* **2003**, *35*, 475−484.
(43) Fukushima, T.; Takemura, H.; Yamashita, T.; Ishisaka, T.; Inai, K.; Imamura, S.; Urasaki, Y.; Ueda, T. *Anticancer Res.* **1999**, *26*, 5111−5115.
(44) Deuchars, K.; Ling, V. P-glycoprotein and multidrug resistance in cancer chemotherapy. *Semin. Oncol.* **1989**, *16*, 156−165.
(45) Hour, T. C.; Chen, C. Y.; Guan, J. Y.; Lu, S. H.; Hsieh, C. Y.; Pu, Y. S. Characterization of chemoresistance mechanisms in a series of cisplatin-resistant transitional carcinoma cell lines. *Anticancer Res.* **2000**, *20*, 3221−3225.
(46) Lampidis, T. J.; Kolonias, D.; Podona, T. ; Israel, M.; Safa, A. R.; Lothstein, L.; Savaraj, N.; Tapiero, H.; Priebe, W. Circumvention of P-GP MDR as a Function of Anthracycline Lipophilicity and Charge Biochem. 1997, *36*, 2679−2685.
(47) Andrews, P. A.; Albright, K. D. Mitochondrial defects in *cis*-diamminedichloroplatinum(II)-resistant human ovarian carcinoma cells. *Cancer Res.* **1992**, *52*, 1895−1901.
(48) Yoon, M. J.; Kim, E. H.; Lim, J. H.; Kwon, T. K.; Choi, K. S. Superoxide anion and proteasomal dysfunction contribute to curcumin-induced paraptosis of malignant breast cancer cells. *Free Radic. Biol. Med.* **2010**, *48*, 713−26.
(49) Hail, N. Jr.; Cortes, M.; Drake, E. N.; Spallholz, J. E. Cancer chemoprevention: a *radical* perspective. *Free Radical Biol. Med.* **2008**, *45*, 97−110.
(50) Ferrari, E.; Saladini, M.; Pignedoli, F.; Spagnolo, F.; Benassi, R. Solvent effect on keto-enol tautomerism in a new β-diketone: a comparison between experimental data and different theoretical approaches. *New J. Chem.* Submitted.
(51) Gutte, B.; Merrifield, R. B. Total synthesis of an enzyme with ribonuclease A activity. *J. Am. Chem. Soc.* **1969**, *91*, 501−502.
(52) Farrugia, L. J. WINGX: An integrated system of widows programs for the solution, refinement and analysis of single-crystal x-ray diffraction data. *J. Appl. Crystallogr.* **1999**, *32*, 837−838.
(53) Szabo, M. R.; Idiţoiu, C.; Chambre, D.; Lupea, A. X. Improved DPPH Determination for Antioxidant Activity Spectrophotometric Assay. *Chem. Pap.* **2007**, *61*, 214−216.
(54) Kueng, W.; Siber, E.; Eppenberger, U. Quantification of cells cultured on 96-well plates. *Anal. Biochem.* **1989**, *182*, 16−19.